Optical constants of $In_{0.53}Ga_{0.47}As/InP$: Experiment and modeling

Martín Muñoz,[a] Todd M. Holden, and Fred H. Pollak[b]
Department of Physics and New York Center for Advanced Technology in Ultrafast Photonic Materials and Applications, Brooklyn College of the City University of New York, Brooklyn, New York 11210

Mathias Kahn and Dan Ritter
Department of Electrical Engineering, Technion-Israel Institute of Technology, Haifa 32000, Israel

Leeor Kronik
Department of Chemical Engineering and Materials Science, University of Minnesota, Minneapolis, Minnesota 55455

Guy M. Cohen
IBM T. J. Watson Research Center, Route 134/P.O. Box 218, Yorktown Heights, New York 10598

(Received 8 July 2002; accepted 28 August 2002)

The optical constants $\varepsilon(E)=\varepsilon_1(E)+i\varepsilon_2(E)$ of unintentionally doped $In_{0.53}Ga_{0.47}As$ lattice matched to InP have been measured at 300 K using spectral ellipsometry in the range of 0.4 to 5.1 eV. The $\varepsilon(E)$ spectra displayed distinct structures associated with critical points at E_0 (direct gap), spin-orbit split $E_0+\Delta_0$ component, spin-orbit split E_1, $E_1+\Delta_1$, E_0' feature, as well as E_2. The experimental data over the entire measured spectral range (after oxide removal) has been fit using the Holden model dielectric function [Holden *et al.*, Phys. Rev. B **56**, 4037 (1997)], plus a Kramers–Kronig consistent correction, described in this work, that improves the fitting at low energies. This extended model is based on the electronic energy-band structure near these critical points plus excitonic and band-to-band Coulomb-enhancement effects at E_0, $E_0+\Delta_0$, and the E_1, $E_1+\Delta_1$, doublet. In addition to evaluating the energies of these various band-to-band critical points, information about the binding energy (R_1) of the two-dimensional exciton related to the E_1, $E_1+\Delta_1$ critical points was obtained. The value of R_1 was in good agreement with effective mass/$\mathbf{k}\cdot\mathbf{p}$ theory. The ability to evaluate R_1 has important ramifications for first-principles band-structure calculations that include exciton effects at E_0, E_1, and E_2 [M. Rohlfing and S. G. Louie, Phys. Rev. Lett. **81**, 2312 (1998); S. Albrecht *et al.*, Phys. Rev. Lett. **80**, 4510 (1998)].
 [DOI: 10.1063/1.1515374]

I. INTRODUCTION

The compound $In_{0.53}Ga_{0.47}As$ lattice matched to InP is of interest from both applied and fundamental perspectives. Structures based on $In_{0.53}Ga_{0.47}As$ materials have been used for several kinds of semiconductor devices, such as heterojunction bipolar transistors,[1–3] resonant tunneling devices,[4] and Bragg reflectors for surface emitting lasers.[5] However, in spite of its fundamental and applied significance, relatively little work has been reported on the optical properties related to the electronic band. Some authors have performed measurements of the $In_{0.53}Ga_{0.47}As$ dielectric function, but have not modeled the experimental results.[6–8] Kelso *et al.*[8] fit the numerical third derivative of the dielectric function, from which the authors were able to obtain the energies of features related to the E_1, $E_1+\Delta_1$ critical points (CPs) (transitions along the equivalent $\langle 111\rangle$ directions of the Brillouin zone). Nee and co-workers[9] modeled the optical constants including the discrete and continuum exciton contributions at E_0 but not at E_1. Adachi[10] modeled the optical constants (0.5–5.5 eV) using the data of Refs. 11 and 12 in the vicinity of E_0, and Ref. 8 in the range of 1.5–5.5 eV. However, his treatment does not include continuum exciton contributions, that is, band-to-band Coulomb enhancement effects (BBCE) at the E_0, $E_0+\Delta_0$, E_1, $E_1+\Delta_1$ CPs.

In this article we report a room temperature spectroscopic ellipsometry (SE) investigation of $\varepsilon(E)[=\varepsilon_1(E)+i\varepsilon_2(E)]$ of unintentionally doped $In_{0.53}Ga_{0.47}As$ in the photon energy range of 0.4 to 5.1 eV. Distinct structures associated with CPs at E_0, spin-orbit split $E_0+\Delta_0$ component, spin-orbit split E_1, $E_1+\Delta_1$ doublet and E_0' feature, as well as E_2, were observed. The experimental data over the entire measured spectral range (after oxide removal) have been fit using the Holden model dielectric function[13] plus a Kramers–Kronig (KK) consistent low energy correction described in this work. This extended model is based on the electronic energy-band structure near these CPs plus discrete and continuum excitonic effects at E_0, $E_0+\Delta_0$, E_1, and $E_1+\Delta_1$. The E_0' and E_2 structures were also included in the analysis. In addition to evaluating the energies of these various band-to-band CPs, it is possible to obtain information about the binding energy (R_1) of the two-dimensional exciton related to the E_1 and $E_1+\Delta_1$ CPs. The obtained value of

[a]Present address: Chemistry Department, City College of the City University of New York, Convent Ave. at 138th Street, New York, NY 10031; electronic mail: mmunoz@sci.ccny.cuny.edu
[b]Also at the Graduate School and University Center of the City University of New York, New York, NY 10036; electronic mail: fhpbc@cunyvm.cuny.edu

R_1 is in reasonable agreement with effective mass/$\mathbf{k}\cdot\mathbf{p}$ theory.[14] The ability to evaluate R_1 has important ramifications for first-principles band-structure calculations, which include exciton effects at E_0, E_1, and E_2.[15,16]

II. EXPERIMENTAL DETAILS

The $In_{0.53}Ga_{0.47}As$ unintentionally doped sample studied was grown on a (001) InP substrate by a compact metalorganic molecular beam epitaxy system.[17] The lattice matching parameter and composition were determined by means of a Philips material research x-ray diffractometer, equipped with Bartels-type four crystal Ge monochromator and a sealed Cu x-ray tube. The residual carrier concentration was evaluated by Hall effect measurements at room temperature to be $n = 1.3\times10^{16}$ cm^{-3}. The optical data in the range of 0.74 to 5.1 eV were taken using a JY-Horiba variable angle phase-modulated ellipsometer. For the interval of 0.4 to 0.9 eV a variable angle instrument, which used a Fourier transform infrared reflectometer as a light source, was employed. Thus, there was some overlap between the two intervals. All the samples were measured with both 65° and 70° incidence angles. To remove the surface oxide an etching procedure was performed. Details are given in Ref. 13, except in this study the etch was a 1:1 mixture of HCl: methanol followed by a quick rinse in methanol and a spray of de-ionized water.

III. EXPERIMENTAL RESULTS

Shown by solid lines in Figs. 1(a) and 1(b) are the experimental values of the real $[\varepsilon_1(E)]$ and imaginary $[\varepsilon_2(E)]$ components of the dielectric function, respectively, as a function of the photon energy. In the ε_2 spectrum there is an absorption edge around 0.75 eV, doublet peaks in the range of 2.5 to 3 eV, and a large feature around 4.5 eV, with some structure on the low energy side around 3.9 eV. A weak feature around 1.1 eV was also observed.

IV. THEORETICAL MODEL

The experimental data over the entire measured spectral range (after oxide removal) has been fit using the Holden model[13] dielectric function plus a correction described in this section that improves the fitting at low energies. This extended model is based on the electronic energy-band structure near these CPs plus excitonic and BBCE effects at E_0, $E_0+\Delta_0$, and the E_1, $E_1+\Delta_1$, doublet.

In the direct-gap zincblende-type semiconductor $In_{0.53}Ga_{0.47}As$ the spin-orbit interaction splits the highest-lying Γ_{15}^v valence band into Γ_8^v and Γ_7^v (splitting energy Δ_0) and the Γ_{15}^c conduction band into Γ_7^c and Γ_8^c (splitting energy Δ_0').[18] The corresponding lowest-lying transitions at $k=0$ [three-dimensional (3D) M_0] are labeled E_0 $[\Gamma_8^v(\Gamma_{15}^v)-\Gamma_6^c(\Gamma_1^c)]$ and $E_0+\Delta_0[\Gamma_7^v(\Gamma_{15}^v)-\Gamma_6^c(\Gamma_1^c)]$, respectively. The spin-orbit interaction also splits the $L_3^v(\Lambda_3^v)$ valence band into $L_{4,5}^v(\Lambda_{4,5}^v)$ and $L_6^v(\Lambda_6^v)$. The corresponding two-dimensional (2D) M_0 CPs are designated $E_1[L_{4,5}^v(L_3^v)-L_6^c(L_1^c)$ or $\Lambda_{4,5}^v(\Lambda_3^v)-\Lambda_6^c(\Lambda_1^c)]$ and $E_1+\Delta_1[L_6^v(L_3^v)-L_6^c(L_1^c)$ or $\Lambda_6^v(\Lambda_3^v)-\Lambda_6^c(\Lambda_1^c)]$, respectively. The E_0', feature corresponds to a transition from the Γ_8^v valence to the spin-orbit split Γ_7^c conduction levels and related transitions along $\langle100\rangle$. The E_2 feature is due to transitions along $\langle110\rangle$ (Σ) or near the X point.[18]

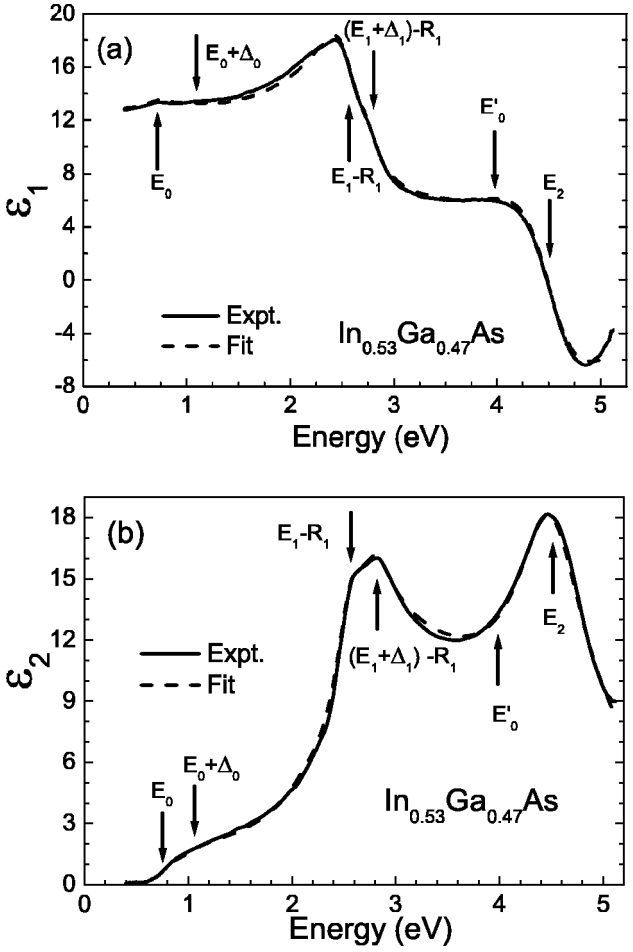

FIG. 1. Solid and dashed lines are the experimental and fit values, respectively, of the (a) real (ε_1) and (b) imaginary (ε_2) components of the complex dielectric function of $In_{0.53}Ga_{0.47}As$.

A. E_0 and $E_0+\Delta_0$ CPs

The data near the E_0 band gap were fit to a function which contains Lorentzian-broadened (a) discrete excitonic (DE) and (b) 3D M_0 BBCE contributions. Pollak and co-workers[19,20] have demonstrated that even if the E_0 exciton is not resolved, the Coulomb interaction still affects the band-to-band line shape. Thus, $\varepsilon_2(E)$ is given by[13]

$$\varepsilon_{2,E_0}(E)=\mathrm{Im}\left\{\frac{A}{E^2}\left[\sum_{q_n=1}^{\infty}\frac{2R_0}{n^3}\left(\frac{1}{E_{n,0}^{\mathrm{ex}}-E-i\Gamma_{n,0}^{\mathrm{ex}}}+\frac{1}{E_{n,0}^{\mathrm{ex}}+E+i\Gamma_{n,0}^{\mathrm{ex}}}\right)+\int_{-\infty}^{\infty}\left(\frac{\theta(E'-E_0)}{1-e^{-2\pi z_1(E')}}-\frac{\theta(-E'-E_0)}{1-e^{-2\pi z_2(-E')}}\right)\frac{dE'}{E'-E-i\Gamma_0}\right]\right\}, \tag{1}$$

where A is a constant, E_0 is the energy of the direct gap, R_0 is the effective Rydberg energy $[=E_0-E_{1,0}^{exc}]$, $E_{n,0}^{\mathrm{exc}}$ and $\Gamma_{n,0}^{\mathrm{exc}}$ are the energy and broadening parameter of the nth state of

the exciton, Γ_0 is the broadening parameter for the band-to-band transition, $z_1(E)=\sqrt{R_0/(E-E_0)}$, $z_2(E)=\sqrt{R_0/(-E-E_0)}$, and $\theta(x)$ is the unit step function. The energy and broadening parameter of the nth exciton state are given by $E_{n,0}^{\mathrm{exc}}=E_0-R_0/n^2$ and $\Gamma_{n,0}^{\mathrm{exc}}=\Gamma_0-(\Gamma_0-\Gamma_{1,0}^{\mathrm{exc}})/n^2$, with n a positive integer. In Eq. (1) the quantity $A \propto R_0^{1/2}\mu_0^{3/2}|P_0|^2$, where μ_0 is the reduced interband effective mass at E_0, and P_0 is the matrix element of the momentum between Γ_8^v–Γ_6^c. The terms in the summation and under the integral in Eq. (1) correspond to the DE and BBCE contributions, respectively.

After the integral calculation Eq. (1) becomes[13]

$$\tilde{\varepsilon}_{E_0}(E)=\frac{A}{2E^2}\left[\sum_{n=1}^{\infty}\{gb_n[\xi(E+i\Gamma_n^{\mathrm{ex}})]+gb_n[\xi(-E-i\Gamma_n^{\mathrm{ex}})]-gb_n[\xi(i\Gamma_n^{\mathrm{ex}})]-gb_n[\xi(-i\Gamma_n^{\mathrm{ex}})]\}+gu[\xi(E+i\Gamma_0)]\right.$$
$$\left.+gu[\xi(-E-i\Gamma_0)]-gu[\xi(i\Gamma_0)]-gu[\xi(-i\Gamma_0)]\right], \tag{2}$$

where

$$\xi^2(X)=\frac{E_0-X}{R},$$
$$gb_n(\xi)=\frac{4}{n^3}\frac{1}{\xi^2-1/n^2}, \tag{3}$$
$$gu(\xi)=-\ln(\xi^2)-\pi\cot\left(\frac{\pi}{\xi}\right)-\sum_{n=1}^{\infty}\frac{2}{n^3}\frac{1}{\xi^2-1/n^2}.$$

However, as pointed out by Schubert *et al.*[21] and illustrated in Fig. 3 of Ref. 13, Eq. (2) has a considerable contribution to ε_2 below the fundamental band gap. In order to improve the low energy behavior of this model we will introduce a KK consistent correction. Considering the first order term in the Taylor series expansion of the imaginary part of the summation corresponding to the bound contributions, given between curly parentheses in Eq. (2), we obtain

$$cgb_0(E,\Gamma^{\mathrm{exc}})=\frac{A}{E}\sum_{n=1}^{\infty}\frac{8\Gamma_n^{\mathrm{exc}}n^3(E_0n^2-R_0)R_0}{[(E_0n^2-R_0)^2+(\Gamma_n^{\mathrm{exc}}n^2)^2]^2}. \tag{4}$$

Note that since $(gb_n[\xi(i\Gamma_n^{\mathrm{ex}})])^*=gb_n[\xi(-i\Gamma_n^{\mathrm{ex}})]$, the sum $gb_n[\xi(i\Gamma_n^{\mathrm{ex}})]+gb_n[\xi(-i\Gamma_n^{\mathrm{ex}})]$ is real and does not make any contribution in our expansion. In a similar way, considering the first order term in the Taylor series expansion of the imaginary part of the sum corresponding to the unbound contributions in Eq. (2), $gu[\xi(E+i\Gamma_0)]+gu[\xi(-E-i\Gamma_0)]$, we obtain

$$cgu_0(E,\Gamma_0)=\frac{A}{E}\left\{\frac{\Gamma_0}{E_0^2+\Gamma_0^2}+\frac{\pi^2}{2R_0}\right.$$
$$\left.\times\mathrm{Im}\left[\frac{1}{\xi^3(i\Gamma_0)}\left(1+\cot^2\left[\frac{\pi}{\xi(i\Gamma_0)}\right]\right)\right]\right\}$$
$$-\frac{1}{2}cgb_0(E,\Gamma_0). \tag{5}$$

Since $gu[\xi(i\Gamma_0)]+gu[\xi(-i\Gamma_0)]$ is real we did not consider it in our expansion. In Eq. (5) the first, second, and third terms between curly parentheses come from the logarithm, cotangent, and sum terms in Eq. (3) respectively. The total correction for the E_0 and $E_0+\Delta_0$ CPs is the sum of Eqs. (4) and (5). In this way the correct line shape for the E_0 and $E_0+\Delta_0$ CPs is

$$\tilde{\varepsilon}_{E_0}(E)=\frac{A}{2E^2}\left[\sum_{n=1}^{\infty}\{gb_n[\xi(E+i\Gamma_n^{\mathrm{ex}})]+gb_n[\xi(-E-i\Gamma_n^{\mathrm{ex}})]-gb_n[\xi(i\Gamma_n^{\mathrm{ex}})]-gb_n[\xi(-i\Gamma_n^{\mathrm{ex}})]\}+gu[\xi(E+i\Gamma_0)]\right.$$
$$\left.+gu[\xi(-E-i\Gamma_0)]-gu[\xi(i\Gamma_0)]-gu[\xi(-i\Gamma_0)]\right]-cgb_0(E,\Gamma^{\mathrm{exc}})-cgu(E,\Gamma_0). \tag{6}$$

The last two terms in this equation have a $1/E$ dependence, and hence their KK transformation is a constant that will be absorbed by $\varepsilon_{1\infty}$, described later.

The $E_0+\Delta_0$ transition has also been described by a function similar to Eq. (6): $\tilde{\varepsilon}_{E_0}(E)\rightarrow\tilde{\varepsilon}_{E_0+\Delta_0}(E)$, $A\rightarrow B$, $E_0\rightarrow E_0+\Delta_0$, $R_0\rightarrow R_{so}$, $\Gamma_{n,0}^{\mathrm{ex}}\rightarrow\Gamma_{n,so}^{\mathrm{ex}}$, and $\Gamma_0\rightarrow\Gamma_{so}$.

Since the exciton at E_0, $E_0+\Delta_0$ has not been resolved, in practice we have used only one exciton, and set $R_0=R_{so}$, $\Gamma_1^{\mathrm{ex}}=\Gamma_0$, and $\Gamma_{0,so}^{\mathrm{ex}}=\Gamma_{so}$.

For $In_{0.66}Ga_{0.34}As$, $R_0=3.5$ meV.[22] According to $\mathbf{k}\cdot\mathbf{p}$ theory[23] $R_0\propto\mu_0$ and hence, using the appropriate electron and heavy hole masses from Ref. 24, we found $R_0=4.0$ meV for our system.

B. E_1 and $E_1+\Delta_1$ CPs

For the E_1 CP, $\varepsilon_2(E)$ is written as[13]

$$\varepsilon_{2,E_1}(E)=\mathrm{Im}\left\{\frac{C_1}{E^2}\left[\sum_{q_n=1}^{\infty}\frac{4R_1}{(2n-1)^3}\left(\frac{1}{E_{n,1}^{\mathrm{ex}}-E-i\Gamma_{n,1}^{\mathrm{ex}}}+\frac{1}{E_{n,1}^{\mathrm{ex}}+E+i\Gamma_{n,1}^{\mathrm{ex}}}\right)\right.\right.$$
$$\left.\left.+\int_{-\infty}^{\infty}\left(\frac{\theta(E'-E_1)}{1-e^{-2\pi z_3(E')}}-\frac{\theta(-E'-E_1)}{1-e^{-2\pi z_4(-E')}}\right)\frac{dE'}{E'-E-i\Gamma_1}\right]\right\}, \tag{7}$$

where C_1 is a constant, E_1 is the energy of the gap, R_1 is the 2D Rydberg energy [$=E_1-E_{1,1}^{\mathrm{exc}}$], $E_{n,1}^{\mathrm{exc}}$ and $\Gamma_{n,1}^{\mathrm{exc}}$ are the energy and broadening parameter, respectively, for the *n*th state of the exciton, Γ_1 is the broadening parameter for the band-to-band transition, $z_3(E)=\sqrt{R_1/(E-E_1)}$, $z_4(E)=\sqrt{R_1/(-E-E_1)}$, and θ(x) is the unit step function. The energy and broadening parameter of the *n*th exciton state are given by $E_{n,1}^{\mathrm{exc}}=E_1-R_1/(2n-1)^2$ and $\Gamma_{n,1}^{\mathrm{exc}}=\Gamma_1-(\Gamma_1-\Gamma_{1,1}^{\mathrm{exc}})/(2n-1)^2$, with n a positive integer.

After the integral calculation Eq. (7) becomes[13]

$$\tilde{\varepsilon}_{E_1}(E)=\frac{C_1}{2E^2}\left[\sum_{n=1}^{\infty}\{gb_n[\xi(E+i\Gamma_n^{\mathrm{ex}})]+gb_n[\xi(-E-i\Gamma_n^{\mathrm{ex}})]\right.$$
$$-gb_n[\xi(i\Gamma_n^{\mathrm{ex}})]-gb_n[\xi(-i\Gamma_n^{\mathrm{ex}})]\}$$
$$+gu[\xi(E+i\Gamma_1)]+gu[\xi(-E-i\Gamma_1)]$$
$$\left.-gu[\xi(i\Gamma_1)]-gu[\xi(-i\Gamma_1)]\right], \tag{8}$$

where

$$\xi^2(X)=\frac{4(E_1-X)}{R_1},$$
$$gb_n(\xi)=\frac{32}{(2n-1)^3}\frac{1}{\xi^2-4/(2n-1)^2}, \tag{9}$$
$$gu(\xi)=-\ln(\xi^2)+\pi\tan\left(\frac{\pi}{\xi}\right)$$
$$-\sum_{n=1}^{\infty}\frac{16}{(2n-1)^3}\frac{1}{\xi^2-4/(2n-1)^2}.$$

For the $E_1+\Delta_1$ CP, a function similar to Eq. (8) was used with $\tilde{\varepsilon}_{E_1}(E)\rightarrow\tilde{\varepsilon}_{E_1+\Delta_1}(E)$, $C_1\rightarrow C_2$, $E_1\rightarrow E_1+\Delta_1$, $R_1\rightarrow R_{1so}$, $\Gamma_{n,1}^{\mathrm{ex}}\rightarrow\Gamma_{n,so}^{\mathrm{ex}}$, and $\Gamma_1\rightarrow\Gamma_{1so}$.

In practice we have used only one exciton and set $R_1=R_{1so}$, $\Gamma_1^{ex}=\Gamma_1$, and $\Gamma_{1,so}^{\mathrm{ex}}=\Gamma_{1so}$. It is possible to find a correction similar to Eq. (5) for the E_1 and $E_1+\Delta_1$ CPs. However, due to the strong intensity of these transitions, even using this correction they produce some considerable contribution below the band gap. Hence, for these transitions, as well as the higher order ones, we apply the linear cutoff correction described below.

Due to the relatively large values of R_1 ($\approx$30–300 meV),[13,19,20,25,26] the optical structure associated with the E_1, $E_1+\Delta_1$ CPs in diamond- and zincblende-type (DZB) semiconductors are actually mainly the excitonic features E_1-R_1, $E_1+\Delta_1-R_1$, respectively, as denoted in Figs. 1(a), 1(b), 2(a), and 2(b).

C. E_0' and E_2 features

The nature of E_0' and E_2 features is more complicated in relation to E_0, $E_0+\Delta_0$ and E_1, $E_1+\Delta_1$, since they do not correspond to a single, well-defined CP.[18] Therefore, each was described by a damped harmonic oscillator term[13,26]

$$\varepsilon_j(E)=\frac{F_j}{(1-\chi_j^2)-i\chi_j\gamma_j}, \tag{10}$$

with $j=E_0'$ or E_2, where F_j is the amplitude, $\chi_j=E/E_j$, and γ_j is a dimensionless parameter.

The fact that Rohlfing *et al.*[15] found that E_2, like the E_0, $E_0+\Delta_0$ and E_1, $E_1+\Delta_1$ CP features, contains an excitonic component, provides some justification in using a damped oscillator term for this structure.

A constant $\varepsilon_{1\infty}$ was added to the real part of the dielectric constant to account for the vacuum plus contributions from higher-lying energy gaps (E_1', etc.).[13,26] This quantity, which also contains the constant term produced by the KK transformation of Eqs. (4) and (5), should not be confused with the high frequency dielectric constant ε_∞.

In order to reduce the contributions of E_1, $E_1+\Delta_1$, E_0', and E_2 transitions to $\varepsilon_2(E)$ below the fundamental gap E_0 we have introduced a linear cutoff for $\varepsilon_2(E)$, obtaining the corrected imaginary dielectric function $\varepsilon_{2,co}$:

$$\varepsilon_{2,co}(E)=\varepsilon_2(E)\frac{E-E_0}{E_{co}-E_0}, \tag{11}$$

where E_{co} is the cutoff energy and E_0 is the direct band gap. ε_1 was corrected by a numerical KK analysis of Eq. (11). The total dielectric function employed in this work is given by two terms of the Eq. (6)-type corresponding to E_0, $E_0+\Delta_0$ CPs, two terms of the Eq. (8)-type for E_1, $E_1+\Delta_1$ CPs, two terms of the Eq. (10)-type corresponding to E_0' and E_2 features, and $\varepsilon_{1\infty}$ with the proper cutoff correction explained earlier.

The dotted curves in Figs. 1(a) and 1(b) are fits to the experimental data using the model described previously. Ar-

TABLE I. Values of the relevant parameters obtained in this experiment for $In_{0.53}Ga_{0.47}As$ sample. Also listed are energy gaps, broadening parameters, etc., from other investigations

Parameter	This work	Previously reported
$A(eV^{1.5})$	0.160±0.001	1.20[a]
		0.739[b]
E_0(eV)	0.75±0.005	0.749[c]
		0.75[a,d]
R_0(meV)	4.0	2.64[b]
Γ_0, Γ_0^{ex} (meV)	62.0±1.0	
$B(eV^{1.5})$	0.183±0.005	0.3[b]
$E_0+\Delta_0$(eV)	1.05±0.005	1.04[a]
		1.084[b]
Γ_{so}, Γ_{so}^{ex} (meV)	115.0±5.0	
$C_1(eV^2)$	27.212±0.001	
E_1-R_1(eV)	2.568±0.005	2.57[a,e,f]
		2.552[b,e]
R_1(meV)	65.0±10.0	
Γ_1, Γ_1^{ex} (meV)	182.0±5.0	
$C_2(eV^2)$	11.347±0.001	
		2.829[f,g]
$E_1+\Delta_1-R_1$(eV)	2.820±0.005	2.83[a,g]
		2.883[b,g]
Γ_1^{so}, $\Gamma_{1,so}^{ex}$ (meV)	145.0±5.0	
F_0(eV)	2.771±0.005	
E_0'(eV)	3.984±0.01	
γ_0(meV)	782.0±20.0	
F_2(eV)	2.026±0.005	
E_2(eV)	4.512±0.01	4.41[a,h]
γ_2(meV)	182±10	
$\varepsilon_{1\infty}$	2.029±0.002	2.8[a]
E_{co}(eV)	2.116±0.001	

[a]Reference 10.
[b]Reference 9.
[c]Reference 46.
[d]Reference 47.
[e]Incorrectly labeled E_1.
[f]Reference 7.
[g]Incorrectly labeled $E_1+\Delta_1$.
[h]Labeled as E_0'.

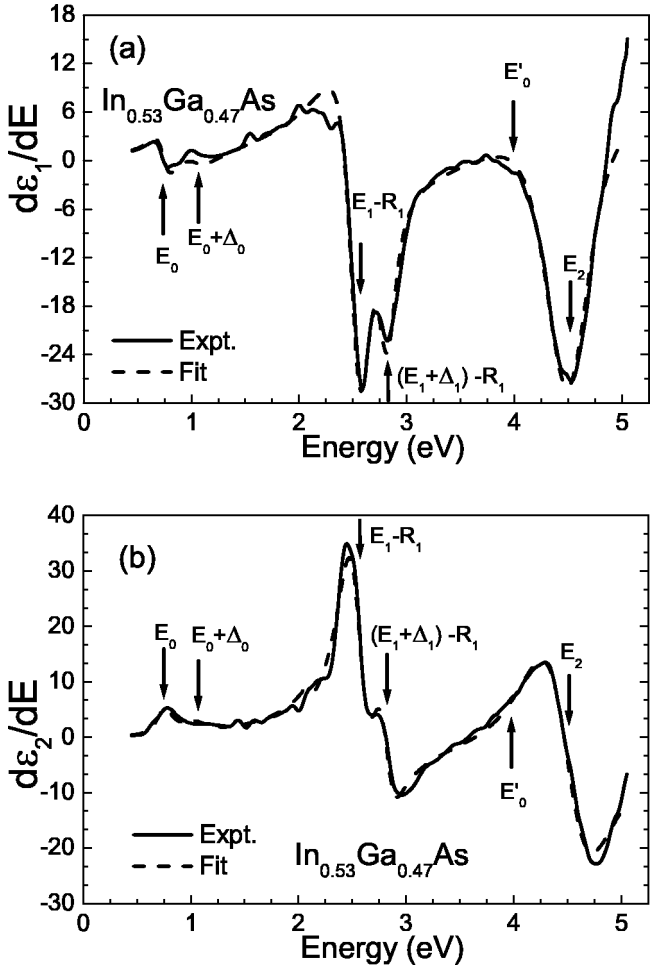

FIG. 2. Solid and dashed lines are the experimental and fit values, respectively, of (a) $(d\varepsilon_1/dE)$ and (b) $(d\varepsilon_2/dE)$ of $In_{0.53}Ga_{0.47}As$.

rows in the various figures indicate the energy values obtained as a result of our fit. All relevant parameters are listed in Table I. The corresponding values of $d\varepsilon_1(E)/dE$ and $d\varepsilon_2(E)/dE$ for the experimental and fit spectra, obtained from a numerical derivative, are shown by the solid and dotted lines in Figs. 2(a) and 2(b), respectively. Overall there is very good agreement between experiment and theory for both the dielectric function [Figs. 1(a) and 1(b)] and the first derivative [Figs. 2(a) and 2(b)].

V. DISCUSSION OF RESULTS AND SUMMARY

The results of this experiment are in good agreement with prior studies of the optical constants of $In_{0.53}Ga_{0.47}As$.[6–8] Figures 1(a) and 1(b) correspond closely to the relevant data of Refs. 6, 7, and 8 in the ranges of 0.65 to 4.96, 1.13 to 3.4, and 1.5 to 5.1 eV, respectively. The real and imaginary components of the index of refraction, n and κ, displayed in Figs. 3(a) and 3(b) respectively, were obtained using our experimental data. Table I shows that the values of the various energy gaps obtained in this investigation, that is, E_0, $E_0+\Delta_0$, E_1-R_1, $E_1+\Delta_1-R_1$, etc., are in good agreement with other selected experiments. There is some scatter in the experimental data, probably due to differences in sample quality, surface preparation and/or line shape analysis. Displayed in Figs. 4(a) and 4(b) are the individual contributions to ε_1 and ε_2, respectively, of the various transitions. The line shape of our absorption coefficient (α) is presented in Fig. 5. The inset in Fig. 5 shows an expanded version of α in the region of the fundamental gap. The absorption coefficient in region of the fundamental band gap $\alpha_x(E)$ has been estimated from a linear interpolation given by[26]

$$\alpha_x(E) = x\alpha_{\mathrm{InAs}}(E+E_0^{\mathrm{InAs}}-E_0^{T(x)}) + (1-x)^*\alpha_{\mathrm{GaAs}}(E+E_0^{\mathrm{GaAs}}-E_0^{T(x)}), \quad (12)$$

where α_i and E_0^i are the absorption and fundamental gap of the relevant end-point materials (i=InAs or GaAs), and $E_0^{T(x)}$ is the fundamental band gap of the ternary $In_xGa_{1-x}As$ of composition x; in our case $x=0.53$. Using the values of E_0^i and optical constants of InAs, and GaAs listed in Ref. 27, we obtain the dashed curve in the inset of Fig. 5. Due to alloy broadening, the experimental α is somewhat larger around the band gap in relation to the linear interpolation.

The optical constants ε_1 and ε_2 for $In_{0.53}Ga_{0.47}As$ over an extended range, have been investigated by a number of authors,[6–12] mainly using SE. However, Dinges *et al.*[6] and Kelso *et al.*[8] did not model their results, although the latter fit the third derivative spectra. In Ref. 10 Adachi used a model

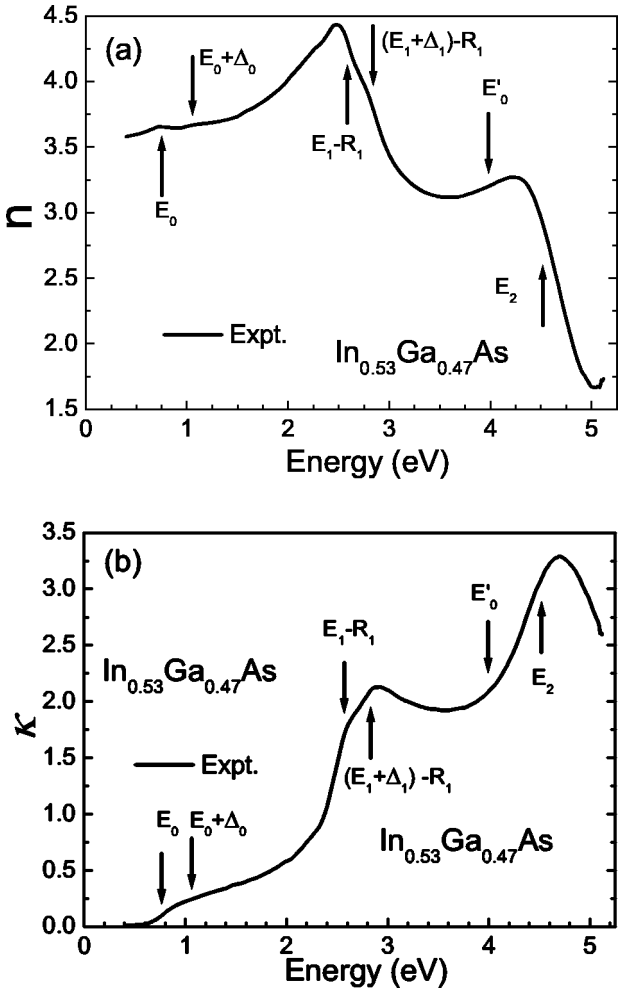

FIG. 3. Solid lines are the experimental values of the (a) real (n) and (b) imaginary (κ) components, respectively, of the complex index of refraction of $In_{0.53}Ga_{0.47}As$.

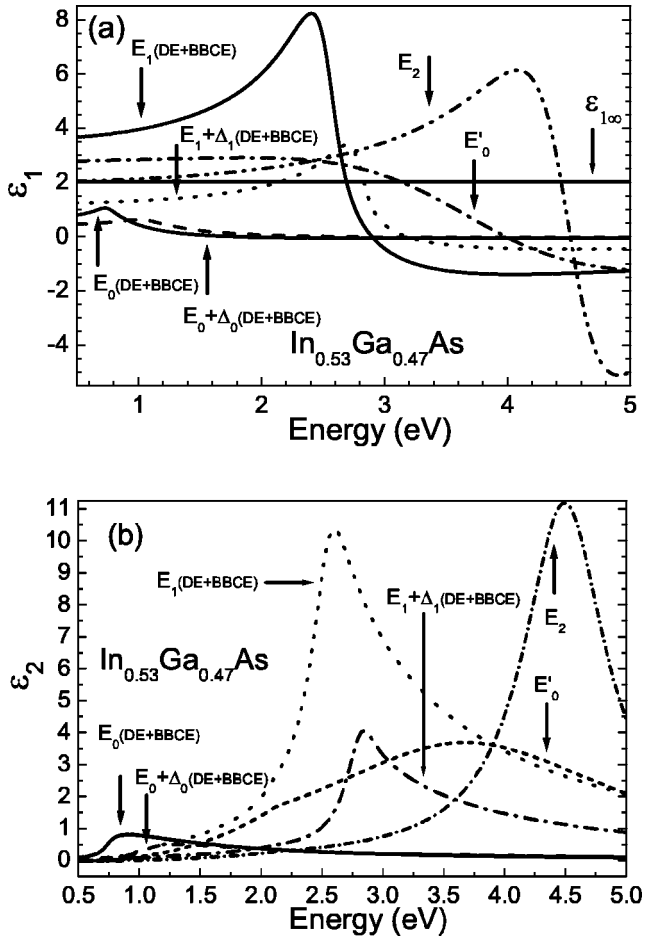

FIG. 4. Individual contributions of the various transitions to (a) ε_1 and (b) ε_2 of $In_{0.53}Ga_{0.47}As$.

in which the E_0, $E_0+\Delta_0$, E_1, and $E_1+\Delta_1$ CPs are represented by only Lorenztian broadened band-to-band single-particle (BBSP) expressions, that is, no DE. As mentioned earlier, the optical structure associated with the E_1 and $E_1+\Delta_1$ CPs is primarily excitonic. In later works, Adachi did include DE terms but with separate amplitude factors for the DE and BBSP contributions.[28,29] However, in the DE plus BBCE approach, for a given CP both terms must have the same strength parameter, for example, $A(E_0)$ and $C_1(E_1)$, as indicated in Eqs. (1) and (7) and in Refs. 13, 20, 26, and 30. In Nee and Green's treatment[9] the BBCE contribution is included at E_0 but not at E_1. Excitonic effects at the E_0 CP also must be included, even at room temperature; in the presence of a DE, the band-to-band E_0 line shape (within about $6-10\,R_0$) is changed from the BBSP square root (broadened) term to a 3D BBCE expression, which has a line shape similar to a step function (broadened) and also increases the amplitude of the absorption in relation to the BBSP expression[13,30–32] Pollak and co-workers[19,20] demonstrated conclusively that even if the exciton at E_0 is not resolved, the line shape is BBCE and not BBSP.

The inadequacy of the BBSP approach at E_0 has been clearly demonstrated in Refs. 19 and 20. These works showed that in the region of the fundamental gap the BBCE term gave a better fit to experimental values of α and $d\varepsilon_2(E)/dE$, respectively, in relation to the BBSP expression. In addition, the nature of BBCE line shape is clearly illustrated in Fig. 6 of Ref. 33, Figs. 2 and 3 of Ref. 34, and by

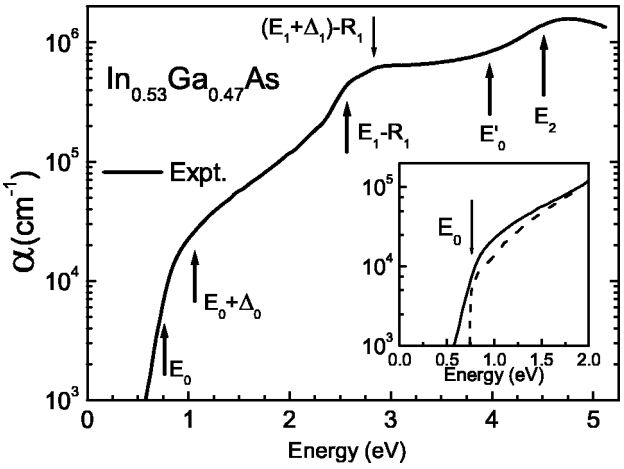

FIG. 5. The solid line is the experimental value of the absorption coefficient α of $In_{0.53}Ga_{0.47}As$. The inset is an expanded version of the experimental data in the region near E_0, the dashed line was calculated from the interpolation scheme based on the end-point materials.

Fig. 3 in Ref. 35. The deficiency of the BBSP model also is elucidated by Figs. 2 and 3 of Ref. 34 and Fig. 3 in Ref. 35. They show that the only use of the BBSP and BBSP plus DE exciton line shapes are not adequate to fit the imaginary part of the dielectric function. In Fig. 3 of Ref. 35 the fit expressions for the DE plus BBSP are considerably lower than the experimental data, particularly for the 21 K measurement.

As mentioned earlier the optical structures associated with the E_1 and $E_1+\Delta_1$ CPs in DZB semiconductors are actually mainly the excitonic features E_1-R_1, $E_1+\Delta_1-R_1$, respectively, as denoted in the figures. Almost all prior optical[8–11] and modulated[36,37] optical studies have incorrectly labeled these excitonic features as "E_1, $E_1+\Delta_1$." Few groups have labeled these features properly.[13,26,28] However, some[28] did not include the BBCE line shape.

Our value of R_1 (65 ± 5 meV) is in good agreement with the effective mass/$\mathbf{k}\cdot\mathbf{p}$ theory of Refs. 14 and 23. According to this approach,

$$R_1=\frac{2\mu_\perp^* e^4}{\hbar^2\varepsilon_\infty^2},$$
$$\frac{1}{\mu_\perp^*}=\frac{1}{m_{c\perp}^*}-\frac{1}{m_{v\perp}^*}, \tag{13}$$

where $\mu_\perp^*$ is the perpendicular reduced interband effective mass related to E_1, and ε_∞ is the high-frequency dielectric function. From a three-band $\mathbf{k}\cdot\mathbf{p}$ formula the perpendicular conduction ($m_{c\perp}^*$) and valence ($m_{v\perp}^*$) effective masses (in units of the free-electron mass) are given by

$$\frac{1}{m_{c\perp}^*}=1+E_P\left(\frac{1}{E_1}+\frac{1}{E_1+\Delta_1}\right),$$
$$\frac{1}{m_{v\perp}^*}=1-\frac{E_P}{E_1}, \tag{14}$$

where E_P is proportional to the square of the magnitude of the matrix element of the perpendicular momentum between the corresponding conduction and valence bands. For GaAs and InAs we have[38] $\varepsilon_\infty(\mathrm{GaAs})=10.9$, $\varepsilon_\infty(\mathrm{InAs})=12.25$, $E_P(\mathrm{GaAs})=25.7$ eV, and $E_P(\mathrm{InAs})=22.2$ eV. From a linear interpolation of these values we obtain $\varepsilon_\infty(\mathrm{In_{0.53}Ga_{0.47}As})=11.62$, $E_P(\mathrm{In_{0.53}Ga_{0.47}As})=23.85$ eV. Using these values, Eq. (13), and our experimental results for E_1, $E_1+\Delta_1$ we found $\mu_\perp^*=0.038$ (in units of the free-electron mass).

For $\mathrm{In_{0.66}Ga_{0.34}As}$, $R_1=55$ meV.[22] From Eq. (13) and a similar linear interpolation we found that for this system $\varepsilon_\infty=11.79$ and $\mu_\perp^*=0.039$. Using these values, the corresponding ones for our system and Eq. (13) we found that R_1 ($\mathrm{In_{0.53}Ga_{0.47}As}$)=55 meV as well. Table II presents the R_1 values for several semiconductors, from which it is possible to appreciate that there is a good agreement between the experimental values and the $\mathbf{k}\cdot\mathbf{p}$ theory. More reliable theoretical values can now be obtained from first-principles band-structure calculations, which include exciton effects.[15,16]

TABLE II. Experimental and calculated values for R_1 for several different semiconductors

Semiconductor	Experiment R_1(meV)	$\mathbf{k}\cdot\mathbf{p}$ theory R_1(meV)
$Zn_{0.53}Cd_{0.47}Se$	270 ± 50[a]	300
CdS	205 ± 30[b]	290
CdTe	145 ± 50[b]	150
$In_{0.66}Ga_{0.34}As$	92 ± 15[c]	55
$In_{0.53}Ga_{0.47}As$	65 ± 10[d]	55
GaSb	32 ± 5[e]	25
$Ga_{0.85}In_{0.15}As_{0.14}Sb_{0.86}$	30 ± 5[f]	25
$Ga_{0.86}In_{0.14}As_{0.14}Sb_{0.86}$	30 ± 5[f]	25

[a]Reference 13.
[b]Reference 19.
[c]Reference 22.
[d]This work.
[e]Reference 26.
[f]Reference 25.

For $\mathrm{In_{0.53}Ga_{0.47}As}$, Adachi[10] obtained a reasonable fit for $\varepsilon_2(E)$, but a poor fit for $\varepsilon_1(E)$, due to the disregarding of the excitonic effects at the E_0, $E_0+\Delta_0$, E_1, and $E_1+\Delta_1$ CPs.

The low energy improvement presented in this work can be appreciated in Fig. 6, which presents in dashed and solid lines the fit curves for $Zn_{0.53}Cd_{0.47}Se$, corresponding to Fig. 3 of Ref. 13, using the Holden model with and without the correction presented in this work. The inset in Fig. 6 represents the region around the fundamental band gap. For this comparison instead of the values A and B reported in Ref. 13, we have used the values $A=1.56$ and $B=1.032$.[39]

The ability to measure R_1 has considerable implications for band-structure calculations, both empirical[18] and first principles.[15,16] In the former case, band-structure parameters, for example, pseudopotential form factors, are determined mainly by comparison with optical and modulated optical experiments, including the "E_1, $E_1+\Delta_1$" features. Therefore, the band-to-band energies are too low by an amount R_1. Rohlfing and Louie have published a first-principles calculation of the optical constants of GaAs, including excitonic effects.[15] Using this formalism they have also calculated R_0.

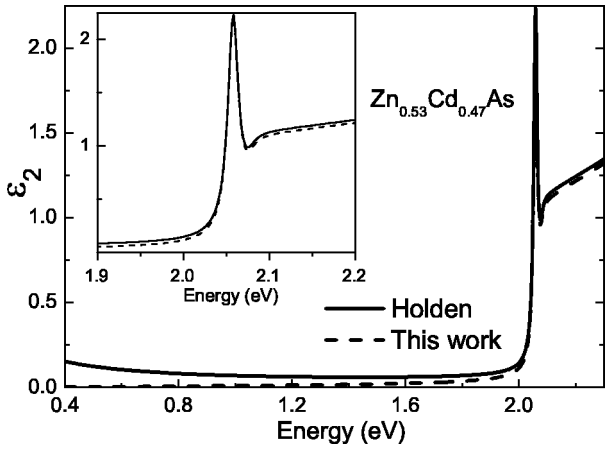

FIG. 6. The dashed and solid lines are the fit for $Zn_{0.53}Cd_{0.47}Se$ using the Holden model with and without the correction presented in this work.

Their approach also makes it possible to evaluate R_1 from first-principles.[40] Albrecht *et al.*[16] have also recently presented an *ab initio* approach for the calculation of excitonic effects in the optical spectra of semiconductors and insulators. However, to date they have presented results for only Si.

The consideration of the excitonic effects at E_0, $E_0+\Delta_0$, E_1, and $E_1+\Delta_1$ during the modeling of the dielectric function is a fundamental consideration, as pointed out by Refs. 41 and 42. Disregarding these effects can produce physically wrong models[43] with the compulsory introduction of additional parameters, like the energy dependent broadening parameter of Refs. 43–45, in order to obtain a somewhat better fit, but without physical meaning.

The low energy KK consistent correction that improves the low energy behavior of the Holden model, which we have introduced in this work, differs from the energy dependent broadening approach of Ref. 44, which contains additional parameters with no physical meaning. When fitting the dielectric function one must bear in mind that all the works discussed above are only ''models.'' All of them make the simplifying assumptions that the dielectric function can be deconstructed into individual contributions from relevant CPs plus related excitonic effects for some of them. The bands are assumed to be completely parabolic. Therefore, one cannot extend these models too far. Clearly, the introduction of additional parameters, such as in Ref. 44, will result in a somewhat better fit.

In summary, we have measured the room-temperature complex dielectric function of bulk $In_{0.53}Ga_{0.47}As$ in the extended range of 0.4 to 5.1 eV using SE. Distinct structures related to CPs associated with the direct gap, spin-orbit split E_0, $E_0+\Delta_0$, spin-orbit split E_1, $E_1+\Delta_1$, E_0' feature, and E_2 have been observed. The experimental data over the entire measured spectral range has been fit using the Holden–Muñoz model for the dielectric function described in this work and based on the electronic energy-band structure near these CPs plus DE and BBCE effects at E_0, $E_0+\Delta_0$, E_1, and $E_1+\Delta_1$. In addition to measuring the energies of these various band-to-band CPs, we have evaluated the 2D exciton binding energy R_1 ($=65\pm5$ meV), in good agreement with effective mass/$\mathbf{k}\cdot\mathbf{p}$ theory. The ability to determine R_1 has important ramifications for first-principles band-structure calculations that have included excitonic effects at various critical points.

ACKNOWLEDGMENTS

Two of the authors (M. M. and F. H. P.) thank the New York State Science and Technology Foundation through its Centers for Advanced Technology program for support of this project. Three of the authors (D. R., M. K., and L. K.) thank the Israel Ministry of Science InP infrastructure program for its support.

[1] T. Kaneto, K. W. Kim, and M. A. Littlejohn, Appl. Phys. Lett. **63**, 48 (1993).
[2] G. L. Belenky, P. A. Garbinski, S. Luryi, M. Mastrapasqua, A. Y. Cho, R. A. Hamm, T. R. Hayes, E. J. Laskowski, D. L. Sivco, and P. R. Smith, J. Appl. Phys. **73**, 8618 (1993).
[3] M. Ohkubo, A. Iketani, T. Ijichi, and T. Kikuta, Appl. Phys. Lett. **59**, 2697 (1991).
[4] J. Singh in *Semiconductor Devices: An Introduction* (McGraw-Hill, New York, 1994).
[5] D. G. Depee, N. D. Gerrard, C. J. Pinzone, R. D. Dupuis, and E. F. Schubert, Appl. Phys. Lett. **56**, 315 (1990).
[6] H. W. Dinges, H. Burkhard, R. Lösch, H. Nickel, and W. Schlapp, Appl. Surf. Sci. **54**, 477 (1992).
[7] H. Burkhard, H. W. Dinges, and E. Kuphal, J. Appl. Phys. **53**, 655 (1982).
[8] S. M. Kelso, D. E. Aspnes, M. A. Pollack, and R. E. Nahory, Phys. Rev. B **26**, 6669 (1982).
[9] T. W. Nee and A. K. Green, J. Appl. Phys. **68**, 5314 (1990).
[10] S. Adachi, Phys. Rev. B **39**, 12612 (1989).
[11] S. Adachi, J. Appl. Phys. **53**, 5863 (1982).
[12] W. Kowalsky, H. H. Wehmann, F. Fiedler, and A. Schlachetzki, Phys. Status Solidi A **77**, K75 (1983).
[13] T. Holden, P. Ram, F. H. Pollak, J. L. Freeouf, B. X. Yang, and M. C. Tamargo, Phys. Rev. B **56**, 4037 (1997).
[14] Y. Petroff and M. Balkanski, Phys. Rev. B **3**, 3299 (1971).
[15] M. Rohlfing and S. G. Louie, Phys. Rev. Lett. **81**, 2312 (1998).
[16] S. Albrecht, L. Reining, R. Del Sole, and G. Onida, Phys. Rev. Lett. **80**, 4510 (1998).
[17] R. A. Hamm, D. Ritter, and H. Temkin, J. Vac. Sci. Technol. A **12**, 2790 (1994).
[18] M. L. Cohen and J. R. Chelikowsky, *Electronic Structure and Optical Properties of Semiconductors* (Springer, Berlin, 1989).
[19] K. Wei, F. H. Pollak, J. L. Freeouf, D. Shvydka, and A. D. Compaan, J. Appl. Phys. **85**, 7418 (1999).
[20] F. H. Pollak, M. Muñoz, T. Holden, K. Wei, and V. M. Asnin, Phys. Status Solidi B **215**, 33 (1999).
[21] M. Schubert, J. A. Woollam, G. Leigiger, B. Rheinländer, I. Pietzonka, T. Saß, and V. Gottschalch, J. Appl. Phys. **86**, 2025 (1999).
[22] T. Holden, F. H. Pollak, J. L. Freeouf, G. W. Charache, and J. E. Raynolds, in Thermophotovoltaic Generation of Electricity, edited by T. J. Coutts, J. P. Renner, and C. S. Allman, AIP Conf. Proc. **460**, 39 (1999).
[23] E. O. Kane, Phys. Rev. **180**, 852 (1969); E. O. Kane, in *Semiconductors and Semimetals*, edited by R. K. Willardson and A. C. Beer (Academic, New York, 1966), Vol. 1, p. 75.
[24] S. H. Pan, H. Shen, Z. Hang, F. H. Pollak, W. Zhuang, Q. Xu, A. P. Roth, R. Masut, C. LeCelle, and D. Morris, Phys. Rev. B **38**, 3375 (1988).
[25] M. Muñoz, K. Wei, F. H. Pollak, J. L. Freeouf, C. A. Wang, and G. W. Charache, J. Appl. Phys. **87**, 1780 (2000).
[26] M. Muñoz, K. Wei, F. H. Pollak, J. L. Freeouf, and G. W. Charache, Phys. Rev. B **60**, 8105 (1999).
[27] E. D. Palik, *Handbook of Optical Constants I* (Academic, New York, 1985); *Handbook of Optical Constants II* (Academic, New York, 1991).
[28] S. Adachi and T. Taguchi, Phys. Rev. B **43**, 9569 (1991).
[29] K. Suzuki and S. Adachi, J. Appl. Phys. **83**, 1018 (1998).
[30] R. J. Elliot, Phys. Rev. **108**, 1384 (1957).
[31] P. Y. Yu and M. Cardona, *Fundamentals of Semiconductors* (Springer, Heidelberg, 1996).
[32] F. Bassani and G. Pastori Parravicini, *Electronic States and Optical Transitions in Solids* (Pergamon, Oxford, 1975).
[33] C. H. Yan, H. Yao, J. M. Van Hove, A. M. Wowchak, P. P. Chow, and J. M. Zavada, J. Appl. Phys. **88**, 3463 (2000).
[34] C. C. Kim and S. Sivananthan, Phys. Rev. B **53**, 1475 (1996).
[35] S. Adachi, Phys. Rev. B **41**, 1003 (1990).
[36] M. Cardona, *Modulation Spectroscopy* (Academic, New York, 1969).
[37] F. H. Pollak and H. Shen, Mater. Sci. Eng., R. **10**, 275 (1993).
[38] *Numerical Data and Functional Relationships in Science and Technology*, Landolt-Bürnstein, p. 102 Tables, Vols. 17a and 17b, edited by O. Madelung, M. Schultz, and H. Weiss (Springer, New York, 1982).
[39] T. Holden (private communication).
[40] S. G. Louie (private communication).
[41] M. Muñoz, F. H. Pollak, and T. Holden, Semicond. Sci. Technol. **16**, 281 (2001).
[42] F. H. Pollak, J. Appl. Phys. **88**, 2175 (2001).
[43] A. B. Djurišić and E. H. Li, Semicond. Sci. Technol. **14**, 958 (1999).
[44] A. B. Djurišić and E. H. Li, J. Appl. Phys. **89**, 273 (2001).
[45] A. B. Djurišić and E. H. Li, J. Appl. Phys. **85**, 2848 (1999).
[46] K. Nakajima, A. Yamaguchi, K. Akita, and T. Kotani, J. Appl. Phys. **49**, 5405 (1976).
[47] Y. Takeda, A. Sasaki, Y. Imamura, and T. Takagi, J. Appl. Phys. **47**, 5405 (1976).